

MR Current Density and Conductivity Imaging: The state of the art.

Michael L. G. Joy

Institute of Biomaterials and Biomedical Engineering and Department of Electrical and Computer Engineering,
University of Toronto, Toronto, Ontario, CANADA M5S 3G9

Abstract—Current Density Imaging (CDI) is an imaging technique that measures electrical current density distributions in a volume of material or tissue, which can be imaged using Magnetic Resonance Imaging (MRI). Measurements of current density are obtained by applying an external current to the material/tissue during an MRI acquisition. The magnetic fields produced by the applied current are mapped onto the phase image of the MRI acquisition. The phase images are processed to compute the current density distribution. Performing CDI requires an MRI system, additional hardware, a modified pulse sequence (PSD) and data processing software. Greig C. Scott, Michael L.G. Joy and R. Mark Henkelman developed CDI in 1988 at the University of Toronto (Canada). The CDI Research Group is presently based at the University of Toronto and is supervised by the author. This paper describes the CDI technique, its applications by this and other groups and recently proposed methods for electrical conductivity imaging based on the technique.

Keywords—Magnetic Resonance Imaging Electrical Current Density Conductivity Impedance

I. INTRODUCTION

A current density image[1] (CDI) is a three dimensional image of electric currents flowing inside the body. These images are of the current density vector and are quantitative. CDI images are made in a magnetic resonance imager (MRI) and do not require any surgery or internal mechanical probes. CDI has the advantage of producing measurements with higher resolution and accuracy deep inside the body than any other current imaging method.

CDI is presently being used to make three-dimensional images of the current distribution created by electrical cardiac defibrillators and other electrotherapy devices in animals. This is expected to allow better electrotherapy devices (like portable heart defibrillators) to be designed.

The basic CDI technique has recently been used to make three-dimensional images of electrical conductivity. These MRI based techniques measure essentially the same parameter as Electrical Impedance Tomography (EIT) but in a significantly different way. For example measurements of surface potentials are not essential for some of these methods. Since the electrical resistance of the tissues (like muscle and brain) changes when they are active and also differs for different tissues, high-resolution EIT images will produce new information about, for example, heart and brain function. Conventional EIT techniques, however, only work well near the body surfaces. The resolution and

accuracy of MR EIT images is expected to remain high deep inside the body.

CDI differs from superconductor quantum interference device (SQUID) based tissue current imaging methods in three significant ways:

- 1) Both methods measure the magnetic fields produced by the current densities of interest. SQUID based measurements, however, are generally not made at points where these currents flow while CDI based measurements are made specifically points where the currents of interest flow.
- 2) At present CDI is insensitive to currents of biological origin due to the low current densities of these currents. A SQUID can detect bio currents.
- 3) At present CDI does not have as high a temporal resolution as SQUID.

The ability of MRI to measure magnetic fields inside the body provides a fundamental advantage when solving inverse problems of current and conductivity imaging.

II. METHODOLOGY

A. Current Density Imaging

CDI uses the MR imager to measure the magnetic vector field, \mathbf{B} , produced by volume currents inside the region where the current is flowing. This magneto metric technique is common to all the current and conductivity imaging methods discussed in this paper. The CD vector, \mathbf{J} , is computed using Maxwell's equation, $\mathbf{J} = \nabla \times \mathbf{B} / \mu_0$. Thus if two or three components of the vector \mathbf{B} are measured in a region then one or three components of the CD can be computed in that region. We have developed three CDI methods.

1. Low frequency CDI (LF CDI) in which the CD varies at "audio frequencies" and the measured component of \mathbf{B} is that parallel to the main MRI static field, \mathbf{B}_0 ,
2. Variable frequency CDI (VF-CDI, AC-CDI) which extends the LF CDI frequency range to about 1 kHz.
3. Radio Frequency CDI (RF CDI) in which the CD varies at the Larmor frequency of the MR Imager and the measured components of \mathbf{B} are those two perpendicular to \mathbf{B}_0 .

These methods differ in the frequencies of the fields \mathbf{B} and \mathbf{B} . The chief advantage of RFCDI over the others is that it allows two components of \mathbf{B} to be measured without reorienting the object being imaged.

B. Low and Variable Frequency Current Density Imaging (LFCDI)[2-4]

The LFCDI MRI pulse sequence is shown schematically in figure 1. It can be constructed from almost any MRI

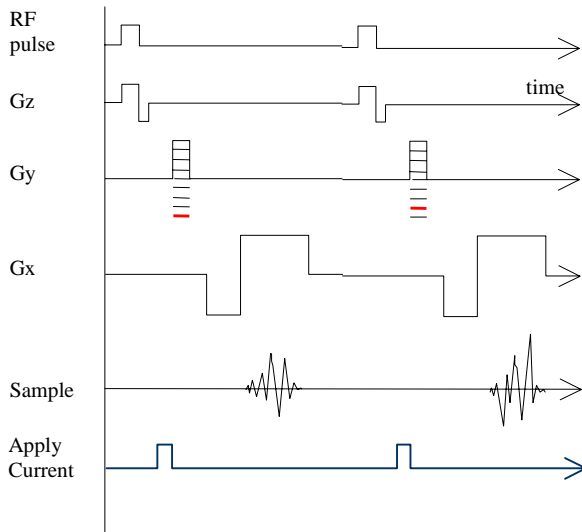


Fig. 1 LFCDI MRI pulse sequence. The externally applied current pulses are synchronized with any standard MR imaging pulse sequence such as the gradient recalled echo sequence shown here.

imaging sequence. It is convenient to use customized pulse generation hardware since a variety of timings and polarities will be employed. Generally a controlled current source is used to ensure that the applied current is not affected by variations in the electrode skin interface resistance. Magnetic resonance images are arrays of complex numbers whose real and imaginary parts are proportional to the x and y components of the nuclear magnetization vector, \mathbf{M} , when the z basis vector is chosen to be parallel to static field, \mathbf{B}_0 . The z component, B_z , of the magnetic field, \mathbf{B} , caused by the current causes \mathbf{M} to precess (rotate) about the z axis at a rate γB_z [Radian/s], where γ is the known gyro magnetic ratio. (The transverse components B_x & B_y have negligible effect on \mathbf{M} .) Thus the phase (argument) of the MR image is equal to the angle, Γ , through which the magnetization rotates as a result of the current pulse. Since the current pulse has a known shape and duration the value of B_z is proportional to Γ . This is the principle used to measure B_z using an MR imager.

Most CDI users[5-19] have used the original spin echo CDI pulse sequence described by Scott [2, 3]. Recently faster gradient recalled echo versions of LFCDI have been implemented[20].

We imaged an AC current pulse using a different approach we called Variable Frequency Current Density Imaging (VFCDI)[4]. Subsequently Mikac developed AC-CDI[21] which also imaged AC current. Both methods require the use of an RF field applied together with the AC

current. In VFCDI this is a constant field whose amplitude times the gyro-magnetic ratio equals the frequency of the applied current. In AC-CDI the applied current is periodically inverted and an RF 180 pulse applied. This approach has the advantage, over the original LFCDI, of reducing loss of signal due to diffusion.

D. Radio Frequency Current Density Imaging (RFCDI)[22-24]

In MRI the magnetization vector, \mathbf{M} , is tipped away from its low energy state parallel to \mathbf{B}_0 by the left circularly polarized (LCP) component of a, radio frequency (RF), magnetic field \mathbf{B} . Only the x y (transverse) components of this field affect \mathbf{M} . Furthermore, the frequency must be close to the Larmor frequency, $\gamma \mathbf{B}_0$. In MRI and LF CDI

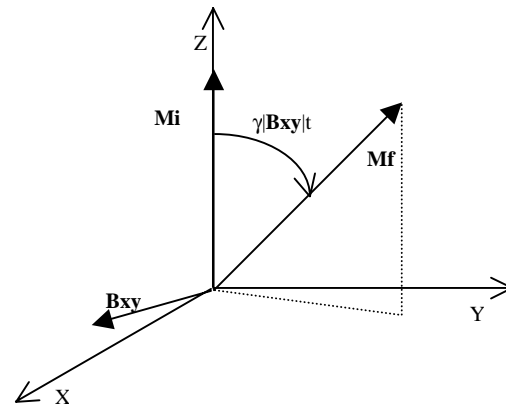


Fig 2: RF CDI in the rotating frame. The LCP, transverse component, B_{xy} , of the magnetic field due to applied RF current causes the nuclear magnetization, \mathbf{M} , to precess at a rate $\gamma|B_{xy}|$ from \mathbf{M}_i to \mathbf{M}_f .

this RF \mathbf{B} is a one of the imaging pulses (e.g. a 90 degree excitation pulse).

In RF CDI the applied current is an RF current. The transverse (x y) left circularly polarized (LCP), \mathbf{B}_{xy} , of the field of this RF current causes \mathbf{M} to precess. The effect of \mathbf{B}_{xy} is best understood by using a left rotating frame of reference in which \mathbf{B}_{xy} appears motionless as is shown in Figure 2. The basic idea behind RFCDI methods is to determine, from MRI phase image(s), the initial and final positions of \mathbf{M} before and after an RF current pulse. For example, in Figure 2, the angle between these two will be proportional to $\gamma|\mathbf{B}_{xy}|$ and their cross product will give the direction of \mathbf{B}_{xy} . In practice inhomogeneity of the static imaging field creates a phase unwrapping problem that has not been satisfactorily solved as yet.

E. MRI Electrical Impedance Tomography (CDI/EIT).

Imaging bio-electric conductivity has long been the goal of Electrical Impedance Tomography (EIT). The goal of EIT is to image the conductivity, σ , of a volume tissue, Ω ,

whose surface is $\partial\Omega$. EIT methods apply electric currents to the surface, $\partial\Omega$, of the volume and measure the consequent electric potential or magnetic field at points on or just

outside the surface. It has been shown that this goal is achievable. The spatial resolution of EIT systems is, however, low at points distant from the surface. This has so far severely limited its medical applications.

Early in its development we realized that CDI might offer an alternative approach to EIT. The simple observation that, in a medium with isotropic conductivity the equipotential surfaces are orthogonal to the measurable current density vectors suggested an EIT method. The potentials of these equipotential surfaces could be determined where they intersected the surface of Ω . There for the electric field, \mathbf{E} , at internal points could be found from the distance, D , between adjacent equipotential surfaces, the potential difference, V , between them and the normalized current density $\mathbf{n} = \mathbf{J}/|\mathbf{J}|$. $\mathbf{E} = V/D \mathbf{n}$. Thus we would know the electric field current density and therefore the assumed isotropic conductivity at all points near these equipotential surfaces. This concept has been explored by Kwon[25] and Eyuboglu[26].

Since CDI measures magnetic fields, \mathbf{B} , produced inside the volume, Ω , by the surface applied currents we saw that it offered information about conditions far from the surface, information unavailable to conventional EIT systems. Furthermore we saw that if we measured the CD at interior points then the potential difference between two surface points, a & b , would be linearly related to the conductivity, σ , by the line integral,

$$V_{ab} = -\int_b^a \left(\frac{1}{\sigma} \right) \mathbf{J} \cdot d\mathbf{l}$$

in which the values of \mathbf{J} were known CD's. This idea was first tested by Zhang [27] who wrote a set of linear equations, $\mathbf{J}\boldsymbol{\rho} = \mathbf{V}$, where \mathbf{J} was a matrix with coefficients obtained from the known CD's and integration path; \mathbf{V} a vector of surface potential differences V_{ab} and $\boldsymbol{\rho}$ a vector of unknown resistivities ($\rho = 1/\sigma$). He attempted to solve this linear inverse problem for all points inside the volume and used straight lines for integration within the volume. From his work he concluded that he could solve a two dimensional problem with a single pair of applied current electrodes. The condition number of his problem rose from 1091 with a large electrode and almost uniform applied current to 24874 with an electrode 400 times smaller (in area). He showed that, with noise, the reconstruction accuracy could be made more uniform by using multiple injection sites to ensure high CD in every voxel for at least one site. His experimental results were not as good as conventional EIT. This was because poor potential measurement technique led to $\pm 10\%$ errors. Simulations

with 10% noise added to the potential gave comparably poor results.

Recently groups have started work on MR EIT methods that do not rely on potential measurements. The first to propose this was Woo[16]. The proposal was to do the CDI experiment and then find a conductivity distribution which produces the same current density distribution as that measured by CDI. This required iteration over each trial conductivity, solving the forward problem for the currents produced by each distribution and then updating the conductivities. Later Ider[28] proposed a similar method in which the measured magnetic field, \mathbf{B} , was compared to magnetic fields computed numerically. It was soon recognized that at least two distinct applications of current were required for a unique solution. This conclusion was later proven recently[29] by the derivation of a simple mathematical expression to compute the gradient of the logarithm of conductivity. An example of initial experimental results is shown in Figure 4. Using this expression and assuming the absolute conductivity of at least one point in the imaged object is known one can obtain the conductivity of other points by integration of the gradient. The iterative algorithm has been refined by Woo's group to the J-substitution algorithm[30].

Subsequent work suggests that knowledge of only a single component of \mathbf{B} for two distinct current applications is required[31, 32].

III. RESULTS

In this section you will find examples of the best images of LFCDI and MR EIT that the authors have produced.

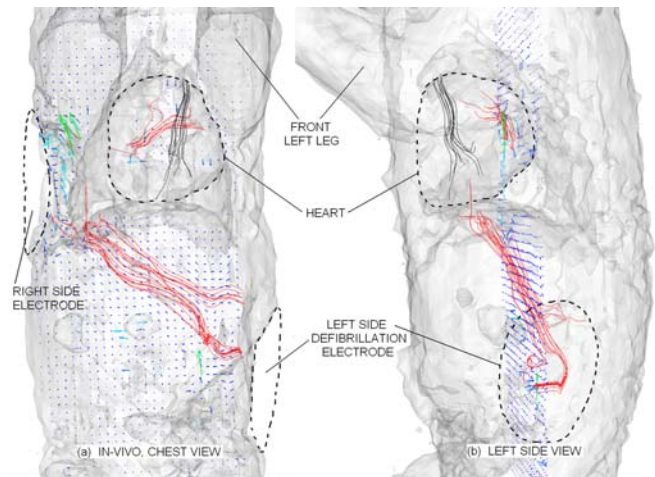


Fig. 3: LFCDI of a live pig (blue arrows). Selected current streamlines between the defibrillation electrodes and within the heart. 1.5 Tesla GE® Signa LX MRI system, 85 mA x 4.6 ms current pulses, effective echo time (TE) of 21 ms, 16 lines of k-space per heart beat (typical heart rate was 115 BPM), spatial encoding of 128 x 128 voxels, field of view (FOV) of 48 x 48 cm, 64 slices, slice thickness of 3.8 mm and a total acquisition time of about 10 min. x 3 orientations = 30 min.

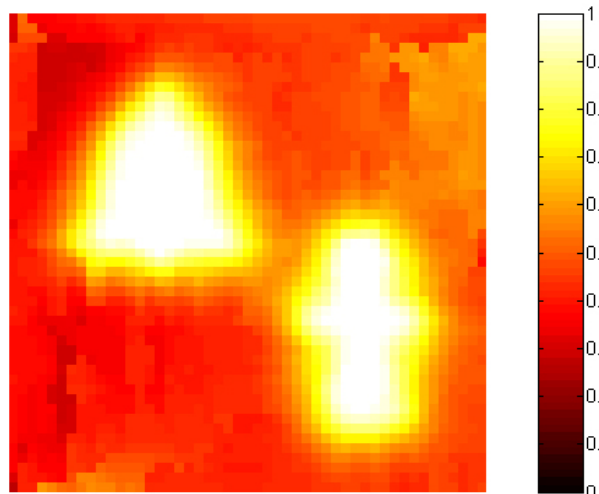


Fig. 4 CDII: Relative conductivity map obtained through integration. Saline filled voids in a conducting gel. A standard LFCDI sequence was employed to measure two current density vector distributions, \mathbf{J}_1 and \mathbf{J}_2 (1.9 mm cubic voxel, TR=3600ms, TE=50ms, Tc=34ms, 2 averages). Each measurement took approximately 19 minutes to complete.[29]. We believe that some of the blur at the edges of the voids is caused by swelling of the gel at the interface with the saline.

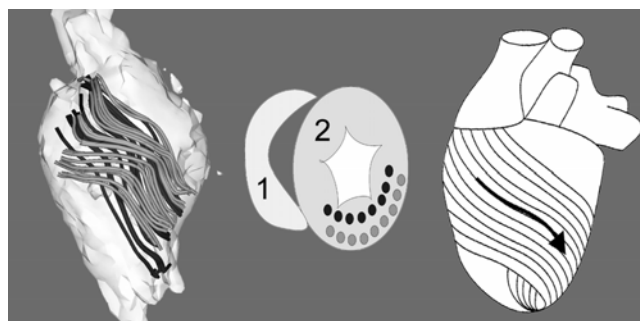


Fig. 5 LFCDI of pig heart after death[13]. Streamlines were seeded inside the left ventricular wall as shown in the center. They seem to follow the cardiac muscle fibers but the deeper seed lines are not parallel to shallow. This suggests that the anisotropy of the muscle strongly affects the current pathways.

The streamlines in figures 1 and 5 are drawn by placing seed points in a specific anatomical region determined from the MR magnitude images which are created with each CDI image. In figure 5 these seed points are separated by <2mm. The noise in the RFCDI image figure 6 is characteristic of RFCDI as mentioned in the introduction.

IV. DISCUSSION

The LF CDI methods are well developed. Fast sequences are producing motion insensitive images in experimental use with live animals. The MR EIT methods all produce current density images as well as conductivity images. However, all ET methods rely on the assumption of isotropic reciprocal conductivity. Since biological tissues are often anisotropic and possibly non reciprocal this could be a problem. Nonetheless, MR EIT images of (mildly)

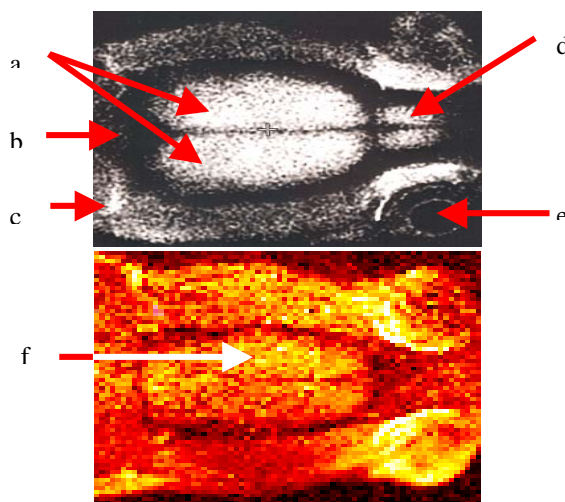


Fig. 6 Top: MRI Magnitude image cortex of rat brain slice. including both hemispheres of the cortex (a), skull (b), fat/muscle/skin (c), occipital cortex (d) and eyes (e). Bottom : RFCDI of he same slice. During unilateral spreading depression (SD) (f).

non-isotropic objects made with these methods do not appear to be severely affected. Thus the older CDI methods will remain in use for some time.

The major problem with all these low frequency methods is that the magnitude of the required applied currents are too high (>5mA) for comfort. This suggests the AC/VFCDI or RFCDI methods should be actively developed. In their present state these non DC methods cannot be used with currents above a threshold that is set by phase unwrapping problem and is not fundamental. Work to design techniques that will allow higher currents to be comfortably and safely used is required.

ACKNOWLEDGMENT

The work described here started with MASc and PhD projects of Greig Scott and reported in his thesis documents and in subsequent papers. This work was first supported by the Natural Sciences and Engineering Council of Canada (NSERC). Subsequent work was supported by both NSERC and The Medical Research Council of Canada (MRC). Presently we are also supported by Philips Medical Systems (Heartstream division), Ontario Research & Development Challenge Fund, General Electric Co, Tyco, Z-tech and Communications and Information Technology Ontario.

The images shown in Figures 1-6 were made possible by: Adrian Nachman, Richard Yoon, Tim Demonte, Karshi Hasanov, Dinghui Wang and Weijing Ma and produced at the Sunnybrook & Women's College Health Sciences Center, Toronto.

REFERENCES

- [1] M. L. G. Joy, G. C. Scott, and R. M. Henkelman, "In-Vivo Detection of Applied Electric Currents by Magnetic Resonance Imaging," *Magnetic Resonance Imaging*, vol. 7, pp. 89-94, 1989.
- [2] G. C. Scott, M. L. G. Joy, R. L. Armstrong, and R. M. Henkelman, "Measurement of nonuniform current density by magnetic resonance," *IEEE Trans. Med. Imag.*, vol. 10, pp. 362-374, 1991.
- [3] G. C. Scott, M. L. G. Joy, R. L. Armstrong, and R. M. Henkelman, "Sensitivity of Magnetic Resonance Current Density Imaging," *J. Mag. Res.*, 1992.
- [4] A. Weinroth, "Variable Frequency Current Density Imaging," in *IBME-Dept of Elec. and Computer Eng.* Toronto: University of Toronto, 1998.
- [5] L. Y. L. Mo, G. Yip, R. S. C. Cobbold, C. Gutt, M. L. G. Joy, G. Santyr, and K. K. Shung, "Non-Newtonian behavior of whole blood in a large diameter tube," *Biorheology*, vol. 28, pp. 421-427, 1991.
- [6] M. L. G. Joy, V. P. Lebedev, and J. Gatti, "Imaging of Current Density and Current Pathways in Rabbit Brain during Transcranial Electrostimulation," *IEEE Trans. Biomed. Eng.*, vol. 46, pp. 1139-1149, 1999.
- [7] T. P. DeMonte, A. Patriciu, M. L. G. Joy, and J. J. Struijk, "Current densities produced by surface electrodes: comparison of MRI measurements and finite element modeling, 2001," presented at ISMRM ,IX'th Sci. Meet. & Exh., Glasgow,686, 2001.
- [8] A. Patriciu, K. Yoshida, T. P. DeMonte, and M. L. G. Joy, "Detecting Skin Burns Induced by Surface Electrodes," presented at 23rd Ann. Int.l Conf. IEEE EMBS, Istanbul,1158, 2001.
- [9] A. Patriciu, T. P. DeMonte, M. L. G. Joy, and J. J. Struijk, "Investigation of Current Densities Produced by Surface Electrodes Using Finite Element Modeling and Current Density Imaging," presented at 23rd Ann.Int.l Conf. IEEE EMBS, Turkey,1157, 2001.
- [10] R. S. Yoon, T. P. DeMonte, D. Jorgenson, and M. L. G. Joy, "Study of current pathways in porcine heart using current density imaging",.," presented at ISMRM ,IX'th Sci. Meet. & Exh., Glasgow,685, 2001.
- [11] T. P. DeMonte, R. S. Yoon, D. Jorgenson, and M. L. G. Joy, "Artifacts Associated with Measuring Cardiac Electrical Currents in a Post-mortem Pig Using Current Density Imaging," presented at ISMRM,X'th Sci. Meet. and Exh.2313, 2002.
- [12] R. S. Yoon, T. P. DeMonte, K. F. Hasanov, D. Jorgenson, and M. L. G. Joy, "Vector Analysis of Current Pathways in Post-mortem Pig Torso," presented at ISMRM,X'th Sci. Meet. and Exh., Honolulu. Hawai'i,2314, 2002.
- [13] R. S. Yoon, T. P. DeMonte, K. F. Hasanov, D. Jorgenson, and M. L. G. Joy, "Direct Measurement of Current Pathways Between Defibrillation Electrodes in a Pig," presented at NASPE 2002, San Diego,697, 2002.
- [14] R. S. Yoon, T. P. DeMonte, K. F. Hasanov, D. B. Jorgenson, and M. L. G. Joy, "Measurement of thoracic current flow in pigs for the study of defibrillation and cardioversion," *Ieee Transactions on Biomedical Engineering*, vol. 50, pp. 1167-1173, 2003.
- [15] R. S. Yoon, T. P. DeMonte, L. Organ, and M. L. G. Joy, "Study of Current Density Distribution in a Non-Invasive Breast Cancer Detection Device," presented at Engineering in Medicine and Biology Soc 25't AIC, Cancun, Mexico,494-496, 2003.
- [16] E. J. Woo, S. Y. Lee, and C. W. Mun, "Impedance tomography using internal current density distribution measured by nuclear magnetic resonance," presented at Mathematical Methods in Medical Imaging III, San Diego, CA, USA,377-385, 1994.
- [17] B. M. Eyuboglu, R. Reddy, and J. S. Leigh, "Imaging of electric current density with MR imaging," *Radiology*, vol. 201, pp. 368-368, 1996.
- [18] B. M. Eyuboglu, R. Reddy, and J. S. Leigh, "Measurement of Electric Current Density with Magnetic Resonance Imaging," presented at Nuclear Science Symposium, Anaheim, CA USA,1472-1473, 1996.
- [19] B. M. Eyuboglu, R. Reddy, and J. S. Leigh, "Imaging electrical current density using nuclear magnetic resonance," *Elektrik*, vol. 6, pp. 201-215, 1998.
- [20] T. P. DeMonte, R. S. Yoon, D. B. Jorgenson, and M. L. G. Joy, "A System for In-Vivo Cardiac Defibrillation Current Density Imaging in a Pig," presented at Engineering in Medicine and Biology Soc 25't AIC, Cancun, Mexico,175-178, 2003.
- [21] U. Mikac, F. Demsar, K. Beravs, and I. Sersa, "Magnetic resonance imaging of alternating electric currents," *Magnetic Resonance Imaging*, vol. 19, pp. 845-856, 2001.
- [22] G. C. Scott, M. L. G. Joy, R. L. Armstrong, and R. M. Henkelman, "RF Current Density Imaging in Homogeneous Media," *Magnetic Resonance in Medicine*, vol. 28, pp. 186-201, 1992.
- [23] G. C. Scott, M. L. G. Joy, R. L. Armstrong, and R. M. Henkelman, "Electromagnetic Considerations for RF Current Density Imaging," *IEEE Transactions on Medical Imaging*, vol. 14, pp. 515-524, 1995.
- [24] G. C. Scott, M. L. G. Joy, R. L. Armstrong, and R. M. Henkelman, "Rotating Frame RF Current Density Imaging," *Magnetic Resonance in Medicine*, vol. 33, pp. 355-369, 1995.
- [25] O. Kwon, J.-Y. Lee, and J.-R. Yoon, "Equipotential line method for magnetic resonance electrical impedance tomography," *Inverse Problems*, vol. 18, pp. 1089-1100, 2002.
- [26] B. M. Eyuboglu, J. S. Leigh, and R. Reddy, "Magnetic Resonance-Electrical Impedance Tomography." United States: The trustees of the University of Pennsylvania, PA (US), 2002.
- [27] N. P. Zhang, "Electrical Impedance Tomography Based on Current Density Imaging," in *IBME & Dept. Electrical Engineering*, 1992.
- [28] Y. Z. Ider and O. Birgul, "Use of the magnetic field generated by the internal distribution of injected currents for Electrical Impedance Tomography (MR-EIT)," *Elektrik*, vol. 6, pp. 215-225, 1998.
- [29] M. L. Joy, A. I. Nachman, K. F. Hasanov, R. S. Yoon, A. W. Ma, M. L. Joy, A. I. Nachman, K. F. Hasanov, R. S. Yoon, and A. W. Ma, "A new approach to Current Density Impedance Imaging (CDII)," presented at ISMRM 12th Scientific Meeting, Kyoto, Japan,2004.
- [30] H. S. Khang, B. I. Lee, S. H. Oh, E. J. Woo, S. Y. Lee, M. Y. Cho, O. Kwon, J. R. Yoon, and J. K. Seo, "J-substitution algorithm in Magnetic Resonance Electrical Impedance Tomography (MREIT): Phantom experiments for static resistivity images," *IEEE Transactions on Medical Imaging*, vol. 21, pp. 695-702, 2002.
- [31] O. Birgul, B. M. Eyuboglu, and Y. Z. Ider, "Experimental results for 2D magnetic resonance electrical impedance tomography (MR-EIT) using magnetic flux density in one direction," *Physics in Medicine and Biology*, vol. 48, pp. 3485-3504, 2003.
- [32] S. H. Oh, B. I. Lee, E. J. Woo, S. Y. Lee, M. H. Cho, O. Kwon, and J. K. Seo, "Conductivity and current density image reconstruction using harmonic B-z algorithm in magnetic resonance electrical impedance tomography," *Physics in Medicine and Biology*, vol. 48, pp. 3101-3116, 2003.